



Cite this: *Soft Matter*, 2019, 15, 433

# Poly(vinyl alcohol)-induced thixotropy of an L-carnosine-based cytocompatible, tripeptidic hydrogel†

Rita Das Mahapatra, <sup>a</sup> Joykrishna Dey <sup>\*a</sup> and Richard G. Weiss <sup>b</sup>

The generally poor mechanical stability of hydrogels limits their use as functional materials for many biomedical applications. In this work, a poly(vinyl alcohol) (PVA) embedded hybrid hydrogel of a  $\beta$ -amino acid-containing Fmoc-protected tripeptide was produced at physiological pH (7.4) and room temperature. The hydrogel system was characterized by a number of techniques, including UV-vis, fluorescence, circular dichroism, FT-IR spectroscopy, electron microscopy, and rheology. While the tripeptide-based pure hydrogel was found to be unstable after *ca.* half an hour, addition of PVA, a water soluble polymer, increased the temporal and mechanical stability of the hydrogel. A rheological step-strain experiment demonstrates that the peptide-polymer hydrogel is thixotropic. Results from a fluorescence probe study and transmission electron microscopy reveal that addition of PVA increases both the fibre diameter and entanglement. Circular dichroism spectra of the hydrogels confirm the formation of aggregates with supramolecular chirality. The thixotropic nature of the hydrogel has been exploited to entrap and release doxorubicin, an anticancer drug, under physiological conditions. Furthermore, an MTT assay of the Fmoc-tripeptide using AH927 cells confirmed its cytocompatibility, which broadens the utility of the hybrid gel for biomedical applications.

Received 28th August 2018,  
Accepted 6th December 2018

DOI: 10.1039/c8sm01766b

[rsc.li/soft-matter-journal](http://rsc.li/soft-matter-journal)

## 1 Introduction

In recent years, the increasing range of applications of tunable, stimuli-responsive and robust gels, especially hydrogels,<sup>1–10</sup> of low-molecular-mass gelators (LMMGs) in fields such as sensors, biomaterials, tissue engineering, and drug delivery has attracted the attention of chemists, physicists, materials scientists, and engineers. However, tenability is frequently found at the expense of another important attribute, gel toughness; many of the gels are observed to be mechanically weak, limiting their utilization in biomedical applications. Especially for site-specific drug delivery vehicles, hydrogels must be mechano-responsive (*i.e.*, thixotropic<sup>11</sup>), such that the gel-to-sol phase transitions can be induced isothermally by mechanical perturbations and the sols reform over time after the cessation of the mechanical force. In principle, thixotropic hydrogels can be used as hosts for injection *in vivo* of guest drug molecules using a syringe to a targeted site. After the removal of the external

stress, the injected solution in the targeted site will recover its gel state, allowing it to remain localised in the targeted area. For this reason, significant efforts have been made to produce hydrogels with the appropriate mechanical properties. However, in spite of those efforts, there are few reports on the use of thixotropic, injectable hydrogels in the field of biomedical applications.<sup>12–18</sup>

In a few previous reports, it has been established that increasing the water solubility of a peptide facilitates stabilization of its fibrils and generates more stable hydrogel systems.<sup>19</sup> In addition, protein/peptide co-assembly has also been reported to help in stabilizing the self-assembled structures of the hydrogels.<sup>20–23</sup> Very recently, Nandi and co-workers have demonstrated that incorporation of poly(ethylene glycol) (PEG) into the hydrogel system of *N*-fluorenylmethoxycarbonyl-L-tryptophan improves the mechanical and thixotropic property of the hybrid hydrogel.<sup>24</sup> In fact, amalgamation of polymers as additives with supramolecular gels to modify their characteristics has become a very interesting topic of study.<sup>25</sup>

In this approach, a new robust system is obtained by combining polymers with an externally switchable supramolecular gel so that the new system has excellent mechanical stability while retaining the characteristics of gels. Polymers can interact with the system either by direct interactions with the LMMG fibers by the adsorption of the polymers or indirect interactions

<sup>a</sup> Department of Chemistry, Indian Institute of Technology Kharagpur, Kharagpur-721 302, India. E-mail: joydey@chem.iitkgp.ac.in

<sup>b</sup> Department of Chemistry and Institute for Soft Matter Synthesis and Metrology, Georgetown University, Washington, DC 20057-1227, USA

† Electronic supplementary information (ESI) available: Details of synthesis, chemical identification, and FT-IR, NMR and HRMS spectra of the tripeptide. See DOI: 10.1039/c8sm01766b

by changing the solution viscosity. In 1999, Hanabusa and co-workers first reported an increase of gel strength by the addition of polymers to an LMMG system.<sup>26</sup> They observed that addition of poly(*N*-vinylpyrrolidone) or PEG to a *L*-valine-containing benzene dicarbonyl derivative in 1-propanol enhanced the strength of the resulting gel. A similar enhancement of gel strength in cyclohexane was observed after the addition of polystyrene. However, the reason for these enhancements was unknown. Since then, a number of other reports have appeared. For example, Liu and co-workers have demonstrated that the poly(ethylene-*co*-vinyl acetate) (PEVA) copolymer can induce a dramatic change in the physical appearance and nanostructures of lanosta-8,24-dien-3 $\beta$ -ol:24,25-dihydro-lanosterol (*L/DHL*) gels in diisooctyl phthalate (DIOP).<sup>27</sup> Before adding PEVA, the *L/DHL* system produced opaque gels with needle-like structures, whereas a transparent gel with interconnected branched fibres was obtained after PEVA addition. Later, it was shown that the stability of gels of 4-(4'-ethoxyphenyl) phenyl- $\beta$ -*O*-*D*-glucoside in water/1,4-dioxane mixtures was also enhanced by the addition of poly(2-hydroxyethyl methacrylate) (PHEMA) as a result of the adsorption of the polymer chains onto the growing fibers.<sup>28</sup> Nandi and co-workers have also shown a similar type of enhancement in mechanical strength in chitosan and folic acid gels.<sup>29</sup>

Sometimes, however, addition of a polymer has been shown to weaken a gel. Adams and co-workers have shown that addition of dextran to a pH-dependent naphthalene-dipeptide hydrogel altered the viscosity of the solution, which could be associated with thinner fibers and reduced mechanical strength.<sup>30</sup> The authors attributed the mechanical changes to the increased viscosity of the solution that resulted upon the addition of the polymer; the LMMG molecules were less able to diffuse, leading to decreased mechanical strength. Later, a comparative study on the addition of other polymers such as PEG, poly(vinyl pyrrolidone), and poly(acrylic acid) with LMMG was also performed. Surprisingly, in all cases, the system exhibited decreased mechanical strength.<sup>31</sup> On the other hand, McNeil and co-workers have shown that addition of specifically poly(acrylic acid) to a pyridine-based organogel leads to the generation of thinner fibers, but with increased gel strength and lower critical gelation concentration (CGC) values.<sup>32</sup> Therefore, the outcome of the interaction of a polymer with a gelator is not well-understood. It appears that the choice of gelator and the complementary polymer are important factors in determining whether increased or decreased mechanical strength will be observed.<sup>24,33,34</sup>

It is known that  $\alpha$ -amino acid-containing peptide molecules are susceptible to proteolysis by proteolytic enzymes, a fact that limits the utility of peptide-based hydrogel systems as drug carriers in biomedical applications. For this reason, there is a need for the development of proteolytically-stable peptide hydrogelators. Such stability can be achieved either by introducing one or more *D*-amino acid residues or a  $\beta$ -amino acid into an oligopeptide chain. In a recent report, we have demonstrated an increased proteolytic stability of a number of  $\beta$ -alanine-containing Fmoc-tripeptides that form hydrogels at room temperature at relatively low concentrations.<sup>35</sup> Most of these

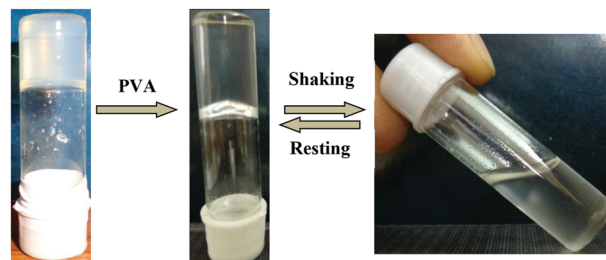
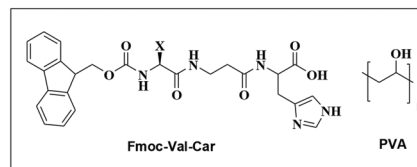


Fig. 1 The appearance of Fmoc-Val-Car hydrogels in the presence and absence of PVA (1% w/v); inset: chemical structures of Fmoc-Val-Car, DOX and PVA.

Fmoc-protected tripeptides, obtained by covalently linking an Fmoc-amino acid to *L*-carnosine (Car, a  $\beta$ -alanine-containing dipeptide), produced mechanically stable hydrogels under physiological conditions. However, one of the tripeptides, containing *L*-valine (Fmoc-Val-Car, Fig. 1), produced a metastable hydrogel which became a sol/solution within half an hour of being formed. Thus, in lieu of the importance of *L*-carnosine-based tripeptide hydrogelators, we report here a study on the effect of a water-soluble polymer on the mechanical strength of the hydrogel produced by the Fmoc-protected tripeptide, Fmoc-Val-Car. By adding poly(vinyl alcohol) (PVA, MW = 89 000–98 000), we have succeeded in increasing the metastability and mechanical strength of the Fmoc-Val-Car hydrogel. The hydrogel was characterized in detail using various techniques, including fluorescence spectroscopy, microscopy and rheology. An MTT assay of the hydrogelator was also performed to determine its cytocompatibility and we studied the entrapment of an anticancer drug, doxorubicin, DOX (Fig. 1), in the peptide/polymer co-assembly, followed by its release kinetics under physiological conditions in order to demonstrate the potential use of the stabilized hydrogel in drug delivery applications.

## 2 Experimental section

### 2.1 Materials

*L*-Carnosine (Car, 99%) and poly(vinyl alcohol) (MW = 89 000–98 000, 99%) were purchased from Sigma-Aldrich (Bangalore, India). Fmoc-*L*-valine (Fmoc-val, 98%), *N*-hydroxysuccinimide (NHS, 98%), and 1,3-dicyclohexylcarbodiimide (DCC, 98%) were purchased from SRL (Mumbai, India) and were used as received. All organic solvents for purification through column chromatography were supplied by SRL (Mumbai, India) and were of the highest purity (99%). Dichloromethane was dried over CaH<sub>2</sub> (SRL, Mumbai) and methanol was dried using I<sub>2</sub>/Mg (SRL, Mumbai) turnings.<sup>35</sup> Milli-Q water (18 M $\Omega$  cm<sup>-1</sup>) was used for the preparation of buffers. The AH927 cells were provided by the Department of Biotechnology, IIT Kharagpur.

Fmoc-Val-Car was synthesized as reported in our previous report and was isolated in the neutral form.<sup>35</sup> The chemical structure of the Fmoc-tripeptide was identified by Fourier transform infrared (FTIR), <sup>1</sup>H-NMR (Fig. S1, ESI<sup>†</sup>), and high-resolution mass spectra (HRMS) (Fig. S2, ESI<sup>†</sup>). Details can be found in the ESI.<sup>†</sup>

## 2.2 Methods and instrumentation

The melting point of the tripeptide was measured using an Instind (Kolkata) melting point apparatus with open capillaries. FT-IR spectra were recorded using a PerkinElmer (Model Spectrum Rx I) spectrophotometer. <sup>1</sup>H NMR spectra were recorded on an AVANCE DAX-400 (Bruker, Sweden) 600 MHz NMR spectrometer in DMSO-*d*<sub>6</sub> solvent.

Aqueous buffer (20 mM, pH 7.4) was made by mixing appropriate volumes of NaH<sub>2</sub>PO<sub>4</sub> and Na<sub>2</sub>HPO<sub>4</sub> solutions. The pH was measured using a digital pH meter (Systronics-335, Kolkata, India) after standardising the instrument with standard pH 7 and pH 4 buffers.

Melting temperatures of the gels were measured by inverting the screw-cap vial (average diameter of 10 mm) containing the gel in a temperature-controlled water bath (JULABO, model F12). The gel was slowly heated at a rate of 1 °C min<sup>-1</sup> until the gelled mass started to flow on tilting of the vial.

The UV-vis spectra of the solutions were recorded using a UV-2450 UV-VIS spectrophotometer (Japan) in a quartz cuvette with a path length of 1 cm. Fluorescence spectra measurements were performed using a 1 cm<sup>2</sup> cuvette on a LS-55 luminescence spectrometer (PerkinElmer, U.K.) equipped with a filter polarizer and a thermostated cell holder. Each sample was equilibrated for 12 h before recording the spectra. The excitation wavelength in all cases was 262 nm and fluorescence was detected at a right angle with respect to the excitation beam.

The morphology of the hydrogels was determined by transmission electron microscopy (TEM), scanning electron microscopy (SEM) and atomic force microscopy (AFM) experiments. TEM images were taken using a transmission electron microscope (FEI-TECNAI G2 20S-TWIN, FEI, USA) operating at an accelerating voltage of 120 kV. The hydrogels were drop cast on carbon-coated copper grids and the samples were air dried. For SEM experiments, the hydrogels were placed on aluminium foil and air-dried at room temperature. A layer of gold was sputtered on top to make a conducting surface, and finally the specimen was transferred into a field emission scanning electron microscope (FESEM, Zeiss, Supra-40, Netherland) operating at 5–10 kV to get the micrograph.

CD spectra were measured on a Jasco J-815 (Japan) spectro polarimeter using quartz cells of 1 mm path length. Samples were equilibrated for 12 h before recording the spectra that were baseline corrected using the appropriate reference solvent.

Rheological measurements were performed on a Bohlin RS D-100 (Malvern, UK) rheometer using the parallel-plate (PP-20, diameter 20 mm) geometry with a constant tool gap of 100 μm. The rheometer was fitted with a solvent trap and a Peltier device that controlled the temperature at 25 ± 0.1 °C. All measurements were performed with matured gels after 10 h

of preparation. Each preformed gel was scooped out from a wide mouth vial using a spatula to avoid damage to the gel structure and was placed on the rheometer plate. An equilibration time of 30 min was allowed for each sample before measurement. Oscillatory stress sweep measurements were carried out at a constant frequency of 1 Hz to obtain storage moduli (*G'*) and loss moduli (*G''*).

The cytotoxicity assay was performed following a standard protocol.<sup>36</sup> AH927 cells were trypsinized and counted using a hemocytometer and then seeded in 96-well micro plates at 5 × 10<sup>4</sup> cells per ml in DMEM (Dulbecco's modified Eagle medium) complete medium. The cells were incubated at 37 °C in 5% CO<sub>2</sub> for 24 h to allow adherence. The medium was replaced with fresh DMEM in the complete medium and incubated with the hydrogelators at concentrations of 20, 50, 100, 200 and 500 μg mL<sup>-1</sup> for 24 h. After incubation, the cells were washed with buffer (pH 7.4) and 100 μL of MTT solution (1 mg mL<sup>-1</sup>) was added to each well. After 3 h of incubation, the MTT solution was removed and replaced with 200 μL of DMSO. Absorbances were recorded at 570 nm using a microplate reader (Thermo Scientific Multiskan Spectrum, USA). Each sample was assayed in triplicate. Control samples include cells with DMSO.

## 3 Results and discussion

### 3.1 Gelation behaviour

Gelation studies of the as-synthesized peptide Fmoc-Val-Car were carried out in 20 mM buffer solutions at different pH values. The results indicate that the peptide is a good hydrogelator at pH 2 and a poor one at pH 7.4. At all other pH values examined, the tri-peptide remained insoluble. Although enhanced solubility of Fmoc-Val-Car at higher pH values is expected to produce larger fibrils, strong inter-fibril interaction can lead to phase separation. This explains why the hydrogel is transparent at pH 2 and translucent at pH 7.4. The detailed gelation properties of Fmoc-Val-Car have been reported in a recent paper from this group.<sup>35</sup> The hydrogel at pH 7.4 was observed to shrink after 30 min by releasing trapped water, but the gel at pH 2 remained unaffected for several days. This unusual behaviour was attributed to either loose packing of the peptide molecules or the hydrophobic nature of the peptide molecules that forced the fibers to phase separate, leaving a supernatant liquid. To enhance the metastability of the hydrogel at pH 7.4, the gelation test of Fmoc-Val-Car was carried out in the presence of different concentrations of a water-soluble polymer, poly(ethylene glycol) (PEG, *M*<sub>w</sub> = 550). However, it failed to stabilize the hydrogel. Thus, we tried another well-known biodegradable polymer,<sup>37</sup> PVA. Because PVA can interact with the gelator molecule through hydrogen-bonds (H-bonds), it was expected to enhance the mechanical stability of the hydrogel. An initial gelation test was performed in the presence of 1% PVA (w/v) at pH 7.4. To our satisfaction, the opaque hydrogel of the tripeptide transformed into a transparent gel that did not flow under the force of gravity over a period of even one month (see Fig. 1). In the presence of 1% PVA, the solubility

of Fmoc-Val-Car in the buffer improved, but it required heating at 60 °C for about 5–10 min to dissolve; in the absence of PVA, heating at 75–80 °C for about 30 min is required for gelation. In order to determine the CGC value and the minimum PVA concentration required to stabilize the hydrogel, a detailed study was carried out. A hydrogel that is stable for more than one month could be obtained in the presence of as little as 0.04% (w/v) PVA. Also the CGC value was observed to decrease from 0.7% (w/v) in pure buffer to 0.5% (w/v) in the presence of 0.04% PVA. Addition of more PVA (4% w/v) led to a further reduction of the CGC of Fmoc-Val-Car to 0.3% (w/v). These data are shown in Fig. 2. The plot shows an initial sharp reduction followed by a slow reduction of the CGC value, indicating very strong co-assembly of the PVA and peptide molecules. In the control experiment involving only 4% PVA in pH 7.4 buffer, however, no gelation was achieved. However, thermo-reversible hydrogel formation by PVA at a very high concentration (15% w/v) induced using a “repeated freezing-and-melting” method has been reported in the literature.<sup>38,39</sup> This leads to the conclusion that a strong interaction between the peptide and the polymer reinforces the Fmoc-Val-Car hydrogel network structure. The phenomenon can be linked to the increased fibre thickness and/or density as a consequence of the stronger H-bonding interactions between the polymer and peptide molecules.

Gelation is believed to be a phenomenon similar to crystallization in which both processes are accompanied by nucleation induced growth.<sup>40–43</sup> Since most nucleation processes are heterogeneous in nature, additives such as dust or other components can modify the nucleation rate by including the additional nucleating sites. In this way, the gelator may produce higher numbers of fibres in the gel network. Alternatively, the higher gel strength may be due to a higher number of nucleating sites and higher fibre density.

The effect of PVA on the thermal stability of the hybrid hydrogels was studied by measuring the gel-to-sol transition temperatures ( $T_{gs}$ ) of the hydrogels prepared in the presence of different concentrations of PVA. The results in Fig. 2 show that

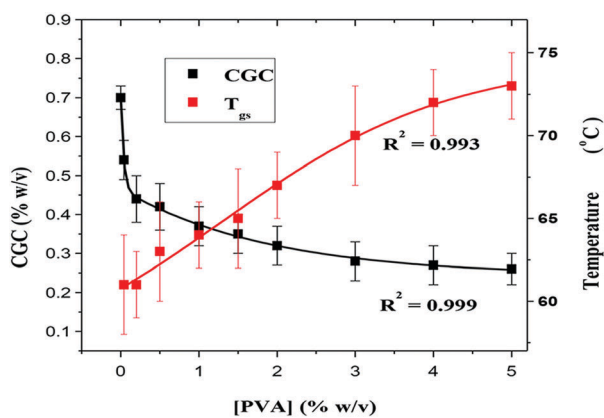


Fig. 2 Variation of CGC and  $T_{gs}$  of Fmoc-Val-Car/PVA hydrogels with increasing [PVA] at 25 °C; the hydrogels were prepared at their respective CGC values.

the thermal stability of the hybrid hydrogel increases non-linearly with [PVA]; there is strong co-assembly of PVA and peptide molecules.

### 3.2 Interaction of Fmoc-Val-Car with PVA

The self-assembly behaviour of Fmoc-Val-Car with and without PVA was monitored by measuring the UV-vis spectra and emission spectra in solution as well as in the gel state (Fig. 3(a)). UV-vis spectra of Fmoc-Val-Car were measured in DMSO and in pH 7.4 buffer solutions. Because the molecules remain in the non-aggregated state in DMSO,<sup>24</sup> the absorption peaks in the range of 290–297 nm can be ascribed to the  $\pi$ - $\pi^*$  transition of the Fmoc moiety. In contrast, when the UV spectra of Fmoc-Val-Car were measured alone in pH 7.4 aqueous buffer solution, a red shift of the peak from 287 to 301 nm was observed. This suggests the existence of  $\pi$ - $\pi$  stacking interactions that facilitate the formation of J-aggregates.<sup>20</sup> However, after the addition of PVA, a small blue shift of the absorption maximum was noticed. This indicates the existence of a significant PVA-peptide interaction which inhibits  $\pi$ - $\pi$  stacking of the Fmoc groups.

The fluorescence emission spectrum of Fmoc-Val-Car in the solution state ( $10^{-6}$  M) was also compared with those of pre-gel solutions of Fmoc-Val-Car ( $3 \times 10^{-3}$  M) with increasing [PVA] as shown in Fig. 3(b). The fluorescence spectrum of Fmoc-Val-Car in the solution state reveals a maximum at 312 nm. However, the fluorescence spectrum of the Fmoc-Val-Car/PVA gel (0.3% PVA) not only experiences a red shift to 327 nm, but also a 2.5 increase in the emission intensity is observed. Furthermore, an increase in the emission intensity (5.8 times) is observed in the Fmoc-Val-Car/PVA gel when the PVA concentration was increased to 1% (w/v), without any further red shift. The red shift in the emission spectra of the hydrogels relative to the solution state clearly confirms the stabilization of the Fmoc groups through extensive  $\pi$ -stacking interaction. This type of rise in emission intensity after the inclusion of polymers is very rare, and only a few reports on this are available in the literature.<sup>24,44</sup> Actually, molecular aggregation through  $\pi$ -stacking interaction causes a decrease in intensity owing to quenching of the excitons by the solvent molecules after gel formation.<sup>45</sup> The rise of fluorescence intensity upon the addition of PVA can be associated with the increase of solution viscosity that prevents free rotation of the Fmoc groups, thereby slowing non-radiative decay processes.

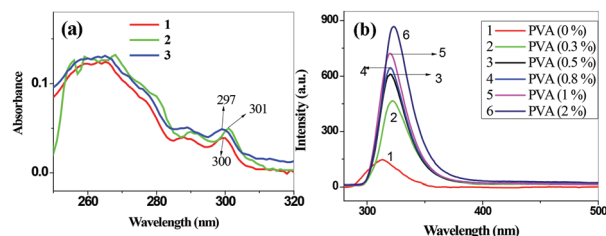


Fig. 3 (a) UV-vis spectra of Fmoc-Val-Car ( $10^{-5}$  M) in buffer (pH 7.4) containing 1% PVA (1), buffer (pH 7.4) without PVA (2) and in DMSO (3); (b) fluorescence spectra of Fmoc-Val-Car with increasing PVA concentration in water. Path length of the cell was 1 mm and  $\lambda_{ex}$  = 265 nm. [Fmoc-Val-Car] for spectrum 1 =  $10^{-6}$  M and [Fmoc-Val-Car] for spectra 2 to 6 =  $3 \times 10^{-3}$  M.

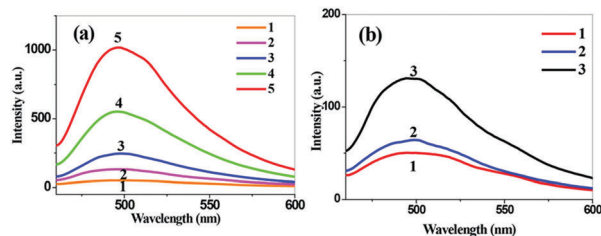


Fig. 4 Fluorescence spectra of thioflavin T (ThT,  $6 \times 10^{-5}$  M) in pH 7.4 buffer as a function of increasing [PVA]: (a) in the presence of Fmoc-Val-Car ( $10^{-5}$  M) (1 = 0 mg, 2 = 0.1 mg, 3 = 0.3 mg, 4 = 0.5 mg, and 5 = 0.7 mg PVA in each 2 mL solution); (b) in the absence of Fmoc-Val-Car but with PVA (1 = 0.1 mg, 2 = 0.5 mg, and 3 = 0.7 mg PVA in each 2 mL solution). The  $\lambda_{\text{ex}}$  and path length of the cell were 440 nm and 1 cm, respectively.

To study the effect of PVA on the network structure of the tripeptide hydrogel, fluorescence measurements (Fig. 4(a)) using thioflavin T (ThT) as a probe were performed at increasing PVA concentrations; this approach is a commonly used method to examine whether fibril formation is occurring during self-assembly:<sup>46–48</sup> an enhancement in ThT fluorescence is an indicator of fibril formation by amphiphilic molecules in solution.<sup>49–51</sup> The experiments were performed at a fixed concentration of Fmoc-Val-Car ( $10^{-5}$  M) and ThT ( $6 \times 10^{-5}$  M) and increasing concentrations of PVA. The fluorescence spectra were recorded by exciting the resultant solutions at 440 nm after equilibrating them for 24 h. The spectra in Fig. 4 show a gradual increase of emission intensity with increasing PVA concentration, suggesting more (or a higher weight fraction of) fibrils upon increasing PVA concentration. Thus, the results as shown in Fig. 4 provide indirect proof that PVA induces formation of fibrils which produce a 3-dimensional (3-D) gel network that entraps increasing amounts of water. Results from a control experiment in which ThT fluorescence was measured in the presence of only PVA, but without any Fmoc-Val-Car (Fig. 4(b)) are consistent with this conclusion; the intensity of ThT fluorescence increases, but to a much smaller extent than when Fmoc-Val-Car is present. The peptide molecules dissolved very easily in the buffer solution, in the presence of PVA. Thus, it appears that PVA interacts with the Fmoc-Val-Car molecules through the formation of additional H-bonds involving its –OH groups. To envisage the participation of all functional groups in the hydrogel formation, FT-IR spectra of Fmoc-Val-Car as a neat solid and as an Fmoc-Val-Car/PVA xerogel were recorded (Fig. S3, ESI<sup>†</sup>). The observed stretching vibrations at 3418 and 3293  $\text{cm}^{-1}$  corresponding to the O–H and N–H vibrations, respectively, in the solid Fmoc-Val-Car are merged, producing a broad peak located at 3435  $\text{cm}^{-1}$  that suggests H-bond formation involving all the functional groups during hydrogelation. The C=O stretching vibration of the –COOH group and the amide groups of solid Fmoc-Val-Car were observed at 1683 and 1654  $\text{cm}^{-1}$ , respectively. After hydrogel formation, these peaks again merged and shifted to 1649  $\text{cm}^{-1}$  with extensive broadening. In the solid sample, a sharp peak of the N–H bending vibration at 1536  $\text{cm}^{-1}$  suffered a reduction in intensity and was not distinguishable after hydrogel formation. Moreover,

to ascertain the H-bond formation between Fmoc-Val-Car and PVA in the hybrid gel state, we have recorded the FTIR spectra of neat PVA (Fig. S3(b), ESI<sup>†</sup>). The spectrum shows the presence of a peak at 3424  $\text{cm}^{-1}$  corresponding to O–H vibrations and is shifted to 3435  $\text{cm}^{-1}$  in the hybrid gel state. Shifting of the O–H vibrations toward higher frequency clearly confirms H-bonding interactions with Fmoc-Val-Car, but not with PVA molecules. Thus, the sum of the spectral changes clearly suggests that intermolecular H-bond formation is one of the principal driving forces for the co-assembly of PVA and Fmoc-Val-Car.

Based on the above results, a model for the incorporation of the two components into the hydrogel network is proposed as shown in Fig. 5. It is based on the aforementioned observations (1) from FTIR spectra that H-bonding interactions develop during gel formation, possibly involving the amide, urethane, –COOH and imidazole groups and (2) from UV-vis absorption and fluorescence spectra that there are  $\pi$ -stacking interactions between the Fmoc groups. In this regard, it is important to remember that the imidazole ring and the –COOH groups in the Fmoc-Val-Car hydrogelator are deprotonated at pH 7.4; the  $\text{p}K_{\text{a}}$  value of the former is  $\sim 6.83$ <sup>52</sup> and that of the latter is 2.64.<sup>52</sup> There should be competition for H-bond formation: (i) the gelator molecules may form intermolecular H-bonds among themselves, leaving PVA intact; (ii) the imidazole and –COO<sup>–</sup> groups may form H-bonds with water molecules; and (iii) PVA can interact with the gelator molecules laterally through H-bonds with the imidazole or –COO<sup>–</sup> groups. Because TEM images (discussed below) suggest that the fibre diameters and density increase after the addition of PVA, we conclude that PVA interacts with the peptide backbone laterally, forming H-bonds with the imidazole and –COO<sup>–</sup> groups. The next layer is added in such a way that the somewhat disordered alkyl chains of PVA create the crystallites observed in the TEM images. As a result, lateral growth of the fibres occurs through H-bond formation with PVA. The longitudinal growth of the fibres, on the

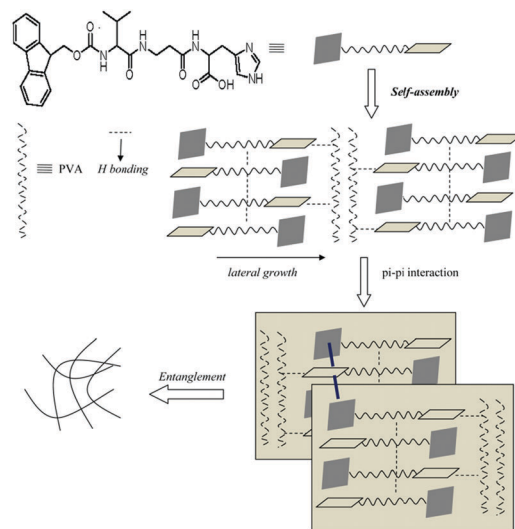


Fig. 5 Schematic model for Fmoc-Val-Car and PVA molecules in the hydrogel.

other hand, occurs through the  $\pi$ -stacking interactions among the Fmoc groups.

### 3.3 Gel morphology

The TEM images of the dried Fmoc-Val-Car hydrogels with and without PVA were recorded to distinguish the differences in gel morphology caused by the presence of the polymer (Fig. 6). In the absence of PVA, the Fmoc-Val-Car gel exhibits fibres with average diameters of  $6 \pm 3$  nm. In the presence of PVA, the fibres tend to entangle to a great extent and there is an increase in fibre diameter that depends on PVA concentration. Also, large PVA crystallites, which act as junction points for fibre growth, form enhanced gelation. The crystallites are formed by the physical cross-linking of the long amorphous chains of PVA.<sup>38</sup> At 0.04% PVA, the fibre diameter was  $15 \pm 5$  nm, whereas at 1% PVA, it increased to  $27 \pm 5$  nm. This increase was accompanied by increased fibre branching (thereby increasing fibre density). These electron micrographs demonstrate that PVA plays a key role in the aggregation processes. Although not very common, this type of increase in fibre diameter after the addition of polymers has been reported by others.<sup>33</sup> Most commonly, a decrease in fibre diameter is found upon the addition of a polymer.<sup>24,29,53</sup> However, the possibility that the change in the network morphology is due to the removal of water during the sample preparation for the TEM cannot be ruled out.

The chiral nature of the Fmoc-Val-Car tripeptide leads to the expectation of chiral, self-assembled supramolecular structures. Unfortunately, insufficient resolution and the effects of drying the samples may have masked any twisting of the fibers. Therefore, circular dichroism (CD) spectra of the hydrogels were recorded to explore the existence of self-assembled structures with supramolecular chirality (Fig. S4, ESI<sup>†</sup>). CD spectra of Fmoc-Val-Car in solution as well as in the hybrid gel containing 1% PVA are reported. In our previous work,<sup>35</sup> it has been shown that no self-assembly occurs in solution at the

$10^{-4}$  M concentration of the gelator. Consequently, the spectrum does not exhibit any discernible signals; the Fmoc groups of molecularly dispersed Fmoc-Val-Car must be able to rotate freely. By contrast, the Fmoc-Val-Car/1% PVA hybrid gel displayed a number of signals, confirming the formation of a more ordered structure in which rotation of the Fmoc group is restricted. The positive peak centred at 230 nm may be indicative of superhelical arrangements of the peptide molecules in the self-assemblies.<sup>54</sup> A number of positive peaks with shoulders between 270 and 305 nm are associated with the  $\pi$ - $\pi^*$  transitions of the Fmoc groups that are stacked face-to-face in the helical aggregates (Fig. S4(a), ESI<sup>†</sup>).<sup>55,56</sup> Even one day after gel preparation, the CD spectrum of the polymer-peptide co-assembly does not exhibit any significant changes. The CD spectrum of the hydrogel in the absence of PVA, recorded immediately after its preparation, shows only one sharp, red-shifted positive peak centred at 305 nm that is indicative of stacking of Fmoc groups. However, this band becomes less prominent with time in a fashion that is correlated with the loss of gel stability.

### 3.4 Thixotropic behavior

The viscoelastic properties of the hydrogels with varying PVA concentrations were determined using oscillatory amplitude and frequency sweep measurements performed at their respective CGC values (Fig. 7). These data allow the yield stress ( $\sigma_y$ ) values of different gels and the impact of PVA on the gel network structure to be compared. The frequency sweep measurements show that the storage modulus ( $G'$ ) is higher than the loss modulus ( $G''$ ) and both remain almost independent of

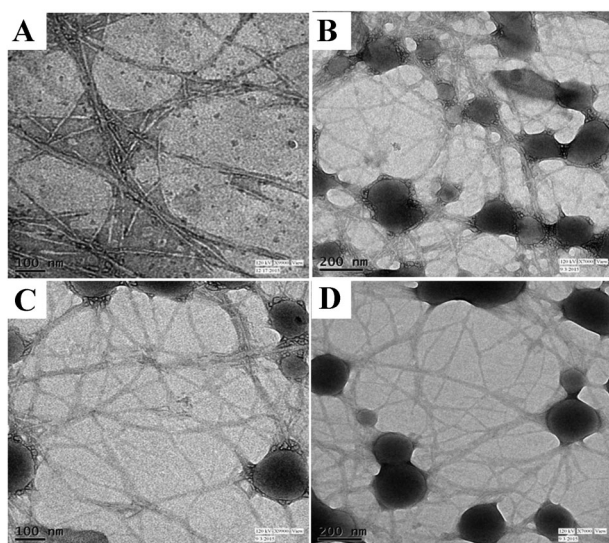


Fig. 6 TEM images of Fmoc-Val-Car (initially  $10^{-4}$  M) solution in the presence of (A) 0% (w/v), (B) 0.04%, (C) 0.5%, and (D) 1% PVA.

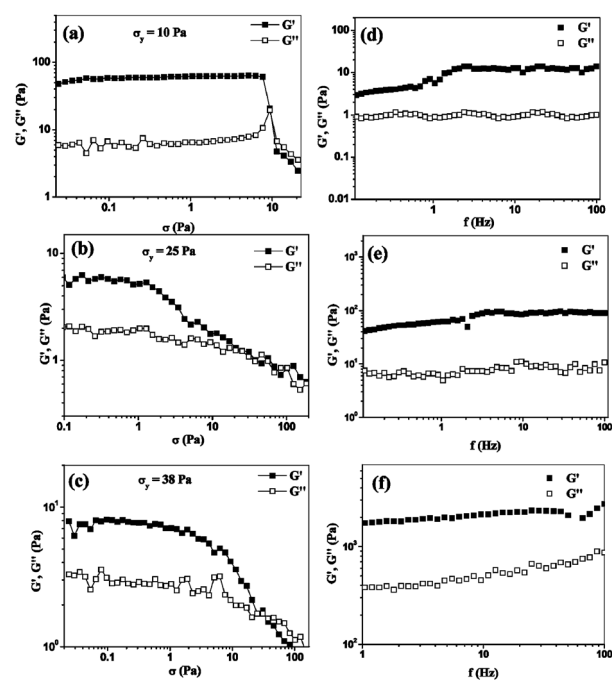


Fig. 7  $G'$  and  $G''$  as a function of shear stress (a–c; frequency = 1 Hz) and frequency (d–f; shear stress = 0.1 Pa) for Fmoc-Val-Car hydrogels at pH 7.4 in the presence of (a, d) 0.1%, (b, e) 0.5%, and (c, f) 1% PVA. The hydrogels were prepared at their respective CGC values.

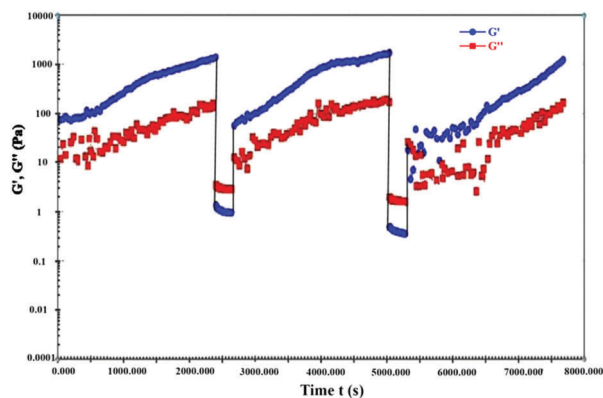


Fig. 8 Continuous measurements at alternating 0.001% and 1% strain (frequency = 1 Hz) for the hydrogel of Fmoc-Val-Car/PVA (1%) at pH 7.4 that had been equilibrated for 12 h before measurements were taken. The hydrogel was prepared at its CGC value.

frequency throughout the range examined; these are hallmarks of a true gel. The  $\sigma_y$  values of the gels were determined in the presence of 0.1, 0.5 and 1% PVA. The increasing order of  $\sigma_y$  values with the increase of [PVA] implies that the hydrogels become mechanically stronger as [PVA] is increased: 10 Pa at 0.1% PVA and 38 Pa at 1% PVA.

The data in Fig. 8 show that the addition of PVA makes the hydrogel thixotropic. Initially, the measurements were made at a minimum strain of 0.001% (*i.e.*, where  $G' > G''$ ). Then, the gel was converted to a viscous-liquid at 1% strain (*i.e.*, where  $G'' > G'$ ). Thereafter, the initial two steps were repeated, leading to small decreases in gel recovery in subsequent cycles. Almost 90% of the gel viscoelasticity was recovered after the first disruption. Based on other studies,<sup>57</sup> it is reasonable to assume that the H-bonding (and other) interactions are being disrupted here when the gels are destroyed mechanically and they are re-established over time when the strain is very small.

### 3.5 Drug encapsulation and release study

The thixotropic nature of the hydrogel is an important property for an injectable drug delivery system. It allows a drug to be encapsulated into a hydrogel matrix isothermally (*i.e.*, avoiding heating and cooling protocols that may affect the drug's efficacy). Also, the drug-encapsulated hydrogel can be converted into a free-flowing solution by mechanical force and then injected using a syringe into the spot where the drug is needed and then the hydrogel will be reconstituted *in vivo* over time. As an example, the anticancer drug, DOX, was encapsulated at  $0.1 \text{ mg mL}^{-1}$  into the hybrid hydrogel matrix utilizing its thixotropic property. Thus, initially 1 mL of a Fmoc-Val-Car/PVA (1%) gel at pH 7.4 was prepared and DOX was encapsulated in it by adding DOX-dissolved buffer on the top of the gel followed by shaking the gel and equilibration of the gel for 12 h to make a homogeneous dispersion of the drug. Then, 1 mL of buffer (pH 7.4) was carefully placed on top of the gel surface (Fig. 9(a)). The release of the drug from the gel matrix to the buffer solution through slow diffusion was monitored *via* UV-vis spectroscopy by measuring the absorbance values at 490 nm at different time intervals.

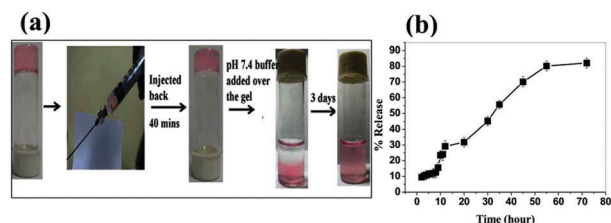


Fig. 9 Release of DOX from an Fmoc-Val-Car/1% PVA hydrogel at pH 7.4: (a) images of the vials during different experimental steps; (b) release profile of DOX from an Fmoc-Val-Car/1%PVA hydrogel at pH 7.4. The concentration of DOX is  $0.1 \text{ mg mL}^{-1}$  and the error bars are calculated using data from two experiments.

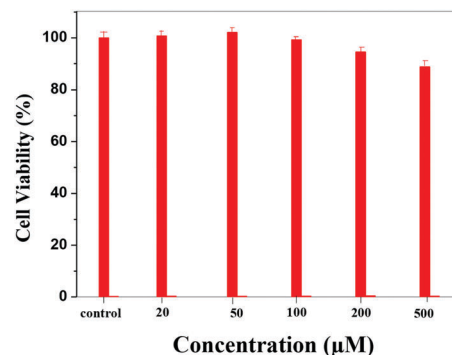


Fig. 10 Cell survival study (by MTT assay) of the hydrogelator Fmoc-Val-Car against the AH 927 cell line.

The release profile thus obtained is presented in Fig. 9(b). The plot indicates that the initial rate of drug release is slow during the first 10 hours, and increases thereafter with a total release of 80% of the drug after 72 hours. Thereafter, the hydrogel became weak and ruptured. The process of drug release initially starts from the surface of the hydrogel by the dissolution of the water-soluble drugs. Then the rest of the drug molecules are released through the diffusion process which is maintained by the penetration of the water molecules into the gel network.<sup>58</sup> From the data in Fig. 9 it appears that the diffusion of water into the gel matrix is a rate-controlling factor.

### 3.6 Cytotoxicity study

An MTT cell viability assay of this hydrogelator Fmoc-Val-Car against AH 927 cells (non-cancerous cells) was performed. The hydrogelator at five different concentrations was incubated with AH 927 cells for 24 h at 37 °C (Fig. 10). The data suggest that all the samples were highly cell compatible; almost 90–95% cells remained alive at the highest concentration of Fmoc-Val-Car, 500  $\mu\text{M}$ , used. Therefore, it can be concluded that the hydrogelator Fmoc-Val-Car and its analogues can be used in biomedical applications.

## 4 Conclusions

The poor mechanical stability of many hydrogels limits their use as functional materials. In this work, a PVA embedded hybrid hydrogel of a tripeptide, Fmoc-Val-Car, was produced in

pH 7.4 buffer and at room temperature. The tripeptide-based hydrogel is not stable for more than half an hour in the absence of added PVA. The room-temperature stability of the hydrogel as well as its mechanical stability increased significantly on the addition of PVA. Structurally, PVA increases both the fibre entanglement and fibre diameter. A fluorescence study indicates that the increase of room-temperature stability of the hydrogel is associated with the higher density of fibres generated. In addition, the addition of PVA imparts a thixotropic behaviour to the peptide hydrogels. The thixotropic nature was utilized to effect the encapsulation and slow release of an anticancer drug, doxorubicin, at physiological pH. An 80% release of doxorubicin from the gel matrix was achieved after 72 hours. Furthermore, the cytocompatibility of the tripeptide Fmoc-Val-Car against AH927 cells broadens the utility of the hydrogel in biomedical applications.

## Conflicts of interest

There are no conflicts to declare.

## Acknowledgements

We thank the Indian Institute of Technology Kharagpur for the partial support of this work. R. D. M. thanks CSIR, New Delhi for a research fellowship (09/081(1157)/2012-EMR-I). The authors are thankful to Dr Kiran Patrui, Department of Agricultural Science, IIT Kharagpur for his assistance with the rheological measurements. We also thank the Department of Biotechnology, IIT Kharagpur for providing AH927 cells and for assistance with the biological measurements. R. G. W. thanks the US National Science Foundation for its support through Grant CHE—1502856.

## Notes and references

- 1 A. Friggeri, B. L. Feringa and J. van Esch, *J. Controlled Release*, 2004, **97**, 241–248.
- 2 J. C. Tiller, *Angew. Chem., Int. Ed.*, 2003, **42**, 3072–3075.
- 3 D.-L. Liu, X. Chang and C.-M. Dong, *Chem. Commun.*, 2013, **49**, 1229–1231.
- 4 J. Chen and A. J. McNeil, *J. Am. Chem. Soc.*, 2008, **130**, 16496–16497.
- 5 X. Wang, A. Horii and S. Zhang, *Soft Matter*, 2008, **4**, 2388–2395.
- 6 A. R. Hirst, B. Escuder, J. F. Miravet and D. K. Smith, *Angew. Chem., Int. Ed.*, 2008, **47**, 8002–8018.
- 7 S. Banerjee, R. K. Das and U. Maitra, *J. Mater. Chem.*, 2009, **19**, 6649–6687.
- 8 A. Dawn, T. Shiraki, S. Haraguchi, S.-i. Tamaru and S. Shinkai, *Chem. – Asian J.*, 2011, **6**, 266–282.
- 9 X. Du, J. Zhou, J. Shi and B. Xu, *Chem. Rev.*, 2015, **115**, 13165–13307.
- 10 D. B. Amabilino, D. K. Smith and J. W. Steed, *Chem. Soc. Rev.*, 2017, **46**, 2404–2420.
- 11 V. A. Mallia and R. G. Weiss, *Soft Matter*, 2016, **12**, 3665–3676.
- 12 A. Pasc, P. Gizzi, N. Dupuy, S. Parant, J. Ghanbaja and C. Gérardin, *Tetrahedron Lett.*, 2009, **50**, 6183–6186.
- 13 H. Liu, Y. Hu, H. Wang, J. Wang, D. Kong, L. Wang, L. Chen and Z. Yang, *Soft Matter*, 2011, **7**, 5430–5436.
- 14 S. Roy, A. Baral and A. Banerjee, *Chem. – Eur. J.*, 2013, **19**, 14950–14957.
- 15 Y. Wang, R. Huang, W. Qi, Z. Wu, R. Su and H. Zhimin, *Nanotechnology*, 2013, **24**, 465603.
- 16 C. Yan, A. Altunbas, T. Yucel, R. P. Nagarkar, J. P. Schneider and D. J. Pochan, *Soft Matter*, 2010, **6**, 5143–5156.
- 17 L. Yu and J. Ding, *Chem. Soc. Rev.*, 2008, **37**, 1473–1481.
- 18 M. Guvendiren, H. D. Lu and J. A. Burdick, *Soft Matter*, 2012, **8**, 260–272.
- 19 D. M. Ryan, T. M. Doran and B. L. Nilsson, *Chem. Commun.*, 2011, **47**, 475–477.
- 20 Y. Kuang, D. Yuan, Y. Zhang, A. Kao, X. Du and B. Xu, *RSC Adv.*, 2013, **3**, 7704–7707.
- 21 D. I. Rożkiewicz, B. D. Myers and S. I. Stupp, *Angew. Chem., Int. Ed.*, 2011, **50**, 6324–6327.
- 22 D. M. Ryan, T. M. Doran and B. L. Nilsson, *Chem. Commun.*, 2011, **47**, 475–477.
- 23 Y. M. Abul-Haija, S. Roy, P. W. J. M. Frederix, N. Javid, V. Jayawarna and R. V. Ulijn, *Small*, 2014, **10**, 973–979.
- 24 P. Chakraborty, S. Mondal, S. Khara, P. Bairi and A. K. Nandi, *J. Phys. Chem. B*, 2015, **119**, 5933–5944.
- 25 D. J. Cornwell and D. K. Smith, *Mater. Horiz.*, 2015, **2**, 279–293.
- 26 K. Hanabusa, A. Itoh, M. Kimura and H. Shirai, *Chem. Lett.*, 1999, 767–768.
- 27 X. Y. Liu and P. D. Sawant, *Angew. Chem., Int. Ed.*, 2002, **41**, 3641–3645.
- 28 M. M. Smith and D. K. Smith, *Soft Matter*, 2011, **7**, 4856–4860.
- 29 P. Chakraborty, B. Roy, P. Bairi and A. K. Nandi, *J. Mater. Chem.*, 2012, **22**, 20291–20298.
- 30 L. Chen, S. Revel, K. Morris, D. G. Spiller, L. C. Serpell and D. J. Adams, *Chem. Commun.*, 2010, **46**, 6738–6740.
- 31 G. Pont, L. Chen, D. G. Spiller and D. J. Adams, *Soft Matter*, 2012, **8**, 7797–7802.
- 32 Y. J. Adhia, T. H. Schloemer, M. T. Perez and A. J. McNeil, *Soft Matter*, 2012, **8**, 430–434.
- 33 P. Chakraborty, S. Das, S. Mondal, P. Bairi and A. K. Nandi, *Langmuir*, 2016, **32**, 1871–1880.
- 34 J. R. Moffat and D. K. Smith, *Chem. Commun.*, 2008, 2248–2250.
- 35 R. Das Mahapatra, J. Dey and R. G. Weiss, *Langmuir*, 2017, **33**, 12989–12999.
- 36 P. Laskar, B. Saha, S. K. Ghosh and J. Dey, *RSC Adv.*, 2015, **5**, 16265.
- 37 A. Takasu, K. Aoki, M. Tsucyia and M. Okada, *J. Appl. Polym. Sci.*, 1999, **73**, 1171–1179.
- 38 E. Yokoyama, I. Masada, K. Shimamura, T. Ikawa and K. Monobe, *Colloid Polym. Sci.*, 1986, **264**, 595–601.
- 39 S. R. Stauffer and N. A. Peppas, *Polymer*, 1992, **33**, 3932–3936.
- 40 M. A. Rogers and A. G. Marangoni, *Langmuir*, 2009, **25**, 8556–8566.

- 41 X. Huang, S. R. Raghavan, P. Terech and R. G. Weiss, *J. Am. Chem. Soc.*, 2006, **128**, 15341–15352.
- 42 G. Tan, V. T. Johnand and G. L. McPherson, *Langmuir*, 2006, **22**, 7416–7420.
- 43 X. Huang, P. Terech, S. R. Raghavan and R. G. Weiss, *J. Am. Chem. Soc.*, 2005, **127**, 4336–4344.
- 44 P. Chakraborty, S. Das, S. Mondal, P. Bairi and A. K. Nandi, *Langmuir*, 2016, **32**, 1871–1880.
- 45 S. Pan, S. Luo, S. Li, Y. Lai, Y. Geng, B. He and Z. Gu, *Chem. Commun.*, 2013, **49**, 8045–8047.
- 46 S. Fleming, S. Debnath, P. W. J. M. Frederix, T. Tuttle and R. V. Ulijn, *Chem. Commun.*, 2013, **49**, 10587–10589.
- 47 R. Vegners, I. Shestakova, I. Kalvinsh, R. M. Ezzell and P. A. Janmey, *J. Pept. Sci.*, 1995, **1**, 371–378.
- 48 A. K. Das, R. Collins and R. V. Ulijn, *Small*, 2008, **4**, 279–287.
- 49 A. Mahler, M. Reches, M. Rechter, S. Cohen and E. Gazit, *Adv. Mater.*, 2006, **18**, 1365–1370.
- 50 R. Orbach, L. Adler-Abramovich, S. Zigerson, I. Mironi-Harpaz, D. Seliktar and E. Gazit, *Biomacromolecules*, 2009, **10**, 2646–2651.
- 51 V. Castelletto, G. Cheng, B. W. Greenland, I. W. Hamley and P. J. F. Harris, *Langmuir*, 2011, **27**, 2980–2988.
- 52 Carnosine. <http://www.druglead.com/cds/carnosine.html>.
- 53 Y. J. Adhia, T. H. Schloemer, M. T. Perez and A. J. McNeil, *Soft Matter*, 2012, **8**, 430–434.
- 54 Z. Yang, H. Gu, Y. Zhang, L. Wang and B. Xu, *Chem. Commun.*, 2004, 208–209.
- 55 D. M. Ryan, T. M. Doran, S. B. Anderson and B. L. Nilsson, *Langmuir*, 2011, **27**, 4029–4039.
- 56 D. M. Ryan, S. B. Anderson, F. T. Senguen, R. E. Youngman and B. L. Nilsson, *Soft Matter*, 2010, **6**, 475–479.
- 57 Y. Zhang and R. G. Weiss, *J. Colloid Interface Sci.*, 2017, **486**, 359–371.
- 58 D. Das, P. Ghosh, S. Dhara, A. B. Panda and S. Pal, *ACS Appl. Mater. Interfaces*, 2015, **7**, 4791–4803.